J Mater Sci (2007) 42:9582–9594
DOI 10.1007/s10853-007-2096-6

Magnetostriction of binary and ternary Fe–Ga alloys

E. M. Summers · T. A. Lograsso · M. Wun-Fogle

Received: 23 May 2007 / Accepted: 10 August 2007 / Published online: 26 August 2007

Abstract This article will review the development of the Fe–Ga (Galfenol) alloy system for magnetostriction applications including work on substitutional ternary alloying additions for magnetic property enhancement. A majority of the alloying addition research has focused on substitutional ternary elements in Bridgman grown single crystals with the intent of improving the magnetostrictive capability of the Galfenol system. Single crystals provide the ideal vehicle to assess the effectiveness of the addition on the magnetostrictive properties by eliminating grain boundary effects, orientation variations, and grain-to-grain interactions that occur when polycrystals respond to applied magnetic fields. In almost all cases, ternary additions of transition metal elements have decreased the magnetostriction values from the binary Fe–Ga alloy. Most of the ternary additions are known to stabilize the $D0_3$ chemical order and could be a primary contribution to the observed reduction in magnetostriction. In contrast, both Sn and Al are found to substitute chemically for Ga. For Sn additions, whose solubility is limited, no reduction in magnetostriction strains are observed when compared to the equivalent binary alloy composition. Aluminum additions, whose effect on the magnetoelastic coupling on Fe is similar to Ga, result in a rule of mixture relationship. The reviewed research suggests that phase stabilization of the disordered bcc structure is a key component to increase the magnetostriction of Fe–Ga alloys.

E. M. Summers
Etrema Products, Inc., Ames, IA 50010, USA

T. A. Lograsso (✉)
Materials and Engineering Physics, 124 Metals Development
Ames Laboratory, Iowa State University, Ames, IA 50014, USA
e-mail: lograsso@ameslab.gov

M. Wun-Fogle
Carderock Division, Naval Surface Warfare Center,
W. Bethesda, MD 20817, USA

Introduction

Over the past few years, there has been an ever-increasing interest in the Fe-Ga (Galfenol) alloy system as a new magnetostrictive smart material for actuator, sensor, and energy harvesting applications. This interest stems from facts that unlike existing smart material systems, Galfenol is the first to offer the combination of good magnetostrictive properties and mechanical properties along with the ability to be formed and welded into various shapes and configurations. In addition, the magnetostriction of Galfenol alloys shows a weak temperature dependence thus allowing Galfenol devices to operate over a wide temperature range without significant changes in performance. Legacy magnetostrictive materials such as iron and nickel provide for mechanically robust smart materials, but they lack the large magnetomechanical responses that applications desire and show strong temperature dependent properties. Conventional piezoceramics, such as PZT and PMN, and rare-earth based magnetostrictives, such as Terfenol-D, offer large strain values, but have limited mechanical robustness which narrows their field of use and also exhibit temperature sensitive properties. A further limitation imposed by the brittleness of these conventional materials is the requirement of operation under compressive loading. In contrast, the good mechanical properties of Fe–Ga alloys and the ability to build in anisotropy through stress annealing, enables Galfenol to operate in the tensile regime without loss of magnetic performance. This ability

truly makes Galfenol a revolutionary material, such that it opens a whole arena for the device engineer to develop unique applications.

The magnetostriction behavior over the entire composition range of Galfenol alloys was established by Clark and co-workers [1] in 2003. An updated plot of magnetostriction values as a function of composition, including data for Fe–Al, is shown in Fig. 1. This curve was created by measuring the saturation magnetostriction of Bridgman grown single crystal samples that had been exposed to homogenizing thermal treatments followed by exposure to various cooling conditions, i.e. furnace cool or quench. Figure 1 shows the existence of two magnetostrictive peaks in the Fe-Ga binary system. The first peak occurring around ~17 to 20 at% Ga depending on the cooling conditions is attributed to two factors: an increase in the magnetoelastic coupling constant (b_1) and softening of the shear modulus, $(C_{11}–C_{12})/2$. The second peak is attributed only to the continued softening in the shear modulus as the magnetoelastic coupling begins to decrease as the Ga content is continually increased from 18.7 at% Ga to 24.1 at% Ga [1]. Magnetostrictions in excess of 400 ppm can be achieved in this system at room temperature under the right processing conditions.

The mechanical and fracture properties of the Fe–Ga alloys have not been studied extensively. Kellogg et al. [2–4] measured mechanical properties of single crystalline $Fe_{83}Ga_{17}$ in tension at room temperature. Yielding began at 0.3% elongation and 450 MPa. An ultimate tensile strength (UTS) of 580 MPa was observed with no fracture occurring through 1.6% elongation. Fracture finally occurred by cleavage along {100} planes. Room temperature mechanical properties [5] of coarse grained polycrystalline FSZM $Fe_{81.6}Ga_{18.4}$ rods were found to be 348–370 MPa UTS with elongation values of 0.81–1.2%. The modulus of elasticity of Fe with 18.4 at% Ga is between 72 and 86 GPa, depending upon FSZM processing conditions. This combination of high magnetostriction and good mechanical properties is rare for more established smart materials.

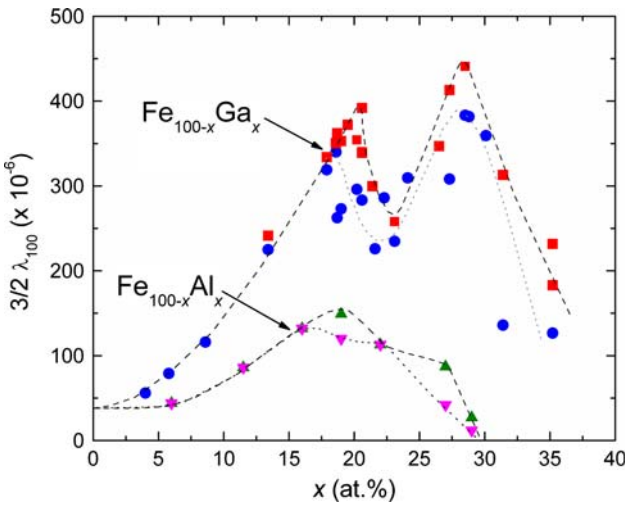

Fig. 1 Magnetostriction constant (3/2) λ_{100} of Fe–Ga and Fe–Al alloys as a function of composition for two heat treated conditions. Samples were annealed in the A2 disordered bcc region and either slow cooled at a programmed rate of 600°/h (blue circles, Fe–Ga alloys; green triangles, Fe–Al alloys) or quenched into water at room temperature (red squares Fe–Ga alloys; magenta inverted triangles, Fe–Al alloys)

This article will review the development of the Galfenol alloy system for magnetostriction applications including work on substitutional ternary alloying additions for magnetic property enhancement. Exploration into Galfenol alloying additions continues to be motivated by the effort to improve the magnetic and mechanical properties of this material. A majority of the alloying addition research has focused on substitutional ternary elements in Bridgman grown single crystals with the intent of improving the magnetostrictive capability of the Galfenol system. Single crystals provide the ideal vehicle to assess the effectiveness of the addition on the magnetostrictive properties by eliminating grain boundary effects, orientation variations, and grain-to-grain interactions that occur when polycrystals respond to applied magnetic fields.

Phase relations in Fe–Ga alloys

A critical component in understanding the magnetoelastic behavior and interpreting the magnetic and physical property measurements are the phase relations and structural variations in the Fe–Ga alloy system. The Fe–Ga phase equilibrium in the region of interest is extremely rich and dynamic. The equilibrium phase diagram [6] for Fe–Ga is shown in Fig. 2. The assessed diagram is based on the work by Köster et al. [7] along with Dasarathy et al. [8] and Bras et al. [9] and is well established. The assessed diagram has recently been verified by Ikeda et al. [10] using diffusion couples and long term annealing (4–21 days).

The terminal bcc phase extends out to about 12 at% Ga at room temperature and as much as 35 at% Ga at ~1050 °C. Fe_3Ga exists at ~27–28 at% Ga as a simple fcc structure ($L1_2$) and undergoes polymorphic transformations on heating first to hexagonal $D0_{19}$ at ~600 °C and then to a $D0_3$ ordered cubic phase at 680 °C. In addition, a B2 ordered cubic phase variant is present at high temperatures for compositions greater than 32 at% Ga.

The determination of the exact nature of the phase relations in the vicinity of Fe–25 at% Ga has been controversial, complicated by the sluggish kinetics of phase formation and metastable phase formation between ~20 at% Ga and 35 at% Ga. On cooling from high

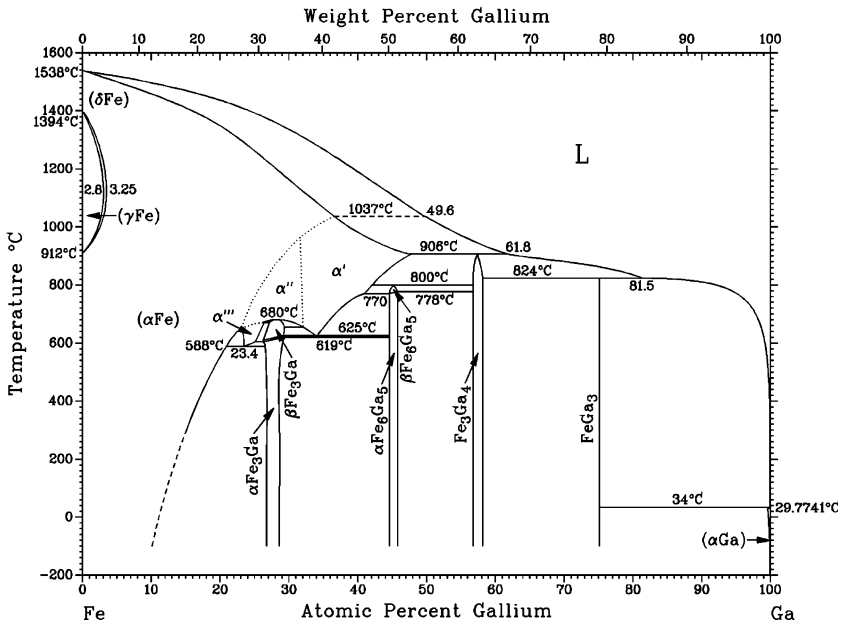

Fig. 2 Equilibrium Fe–Ga phase diagram taken from Ref. 6

temperatures (generally > 1000 °C), the formation of equilibrium phases has been found to be extremely sluggish [7, 9–13]. In particular, the formation of $D0_{19}$ and $L1_2$ ordered phases can be easily avoided during normal cooling rates. Köster et al. [12, 13] and more recently Ikeda et al. [10] have evaluated the phase formation in Fe–Ga at finite cooling rates. Figure 3 is the metastable phase diagram presented by Ikeda and developed using a diffusion couple method which provided a continuous change in composition along the specimen in the compositional range of interest. Their phase diagram is in general agreement with the diagram proposed by Köster et al. [12] who examined the phase distribution following continuous cooling from high temperatures to room temperature.

While the metastable equilibrium diagram appears to simplify phase space, in fact, it has complicated structural determination due to the similarities in lattice parameters and X-ray structure factors of the cubic phases [14]. Figure 4 shows the crystal structures of the three cubic variants. Note that, in the chemically ordered structures, the nearest Ga neighbors lie along differing crystallographic directions, ⟨110⟩ for $D0_3$ and ⟨100⟩ for B2.

Further structural transformations in the Fe–Ga system were explored by Lograsso et al. [14] specifically focusing on single crystal 19 at% Ga specimens that were subjected to various thermal treatments and then analyzed using powder X-ray diffraction. They confirmed the results presented in Refs. 15–17 that by rapidly cooling a 19 at% Ga alloy atomic ordering, i.e. $D0_3$ and/or B2 phase formation, can be prevented. One drawback that is pointed out in Ref. 14 was that using single crystal specimens did not allow for determination of volume fractions or lattice parameters, the former of which is critical to determine any percentage

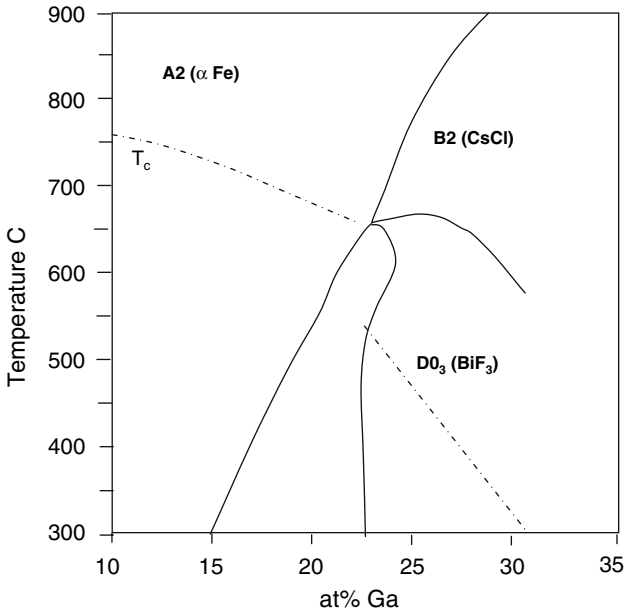

Fig. 3 Metastable Fe–Ga phase diagram redrawn from Ref. 10

ordered phase versus magnetostriction relationship. This lead to further work by Lograsso and Summers [18] in which chill cast polycrystalline samples of 19.5 at% Ga and 22 at% Ga were analyzed using high resolution X-ray diffraction. Due to nearly identical unit cells of the A2 and $D0_3$ phases and similar atomic scattering factors between Fe and Ga quantification of a two phase A2-$D0_3$ phase mixture is problematic due to weak superlattice reflections. However, primary reflections were found to be split and assumed to be caused by the presence of both A2 and $D0_3$ phases. Pseudo-Voight profiles were fitted to the split

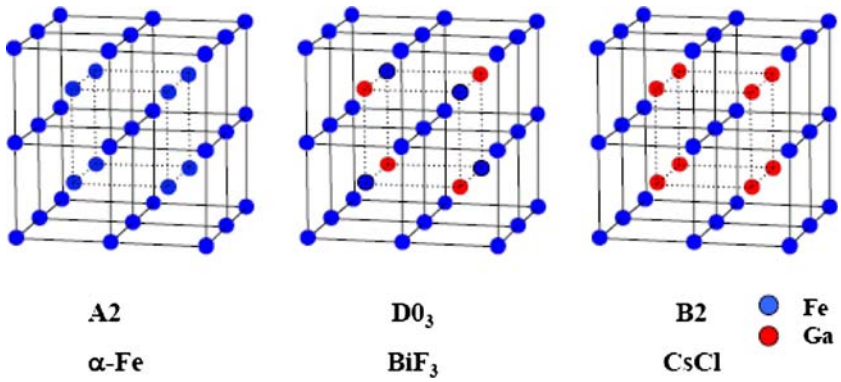

Fig. 4 Representations of the three crystal structures of the cubic variants seen in the Fe–Ga system. Red = Ga locations in the B2 and $D0_3$ structures. For the bcc phase, Fe and Ga can occupy any of the positions

X-ray diffraction peaks as shown in Fig. 5 and from these fits, the volume fraction of each phase was calculated by assuming equivalent structure factors for each phase. For a slow cooled 19 at% Ga alloy, this corresponded to a two-phase mixture of 67.5% A2 and 32.5% $D0_3$. A water quenched 19 at% Ga alloy had no ordered $D0_3$ phase present. Attempts made to apply this technique to highly textured polycrystals in an effort to correlate phase fractions with magnetostriction have not been successful due to the poor counting statistics and a lack of diffraction peaks.

Binary (Fe–Ga) magnetostrictive system

R.C. Hall conducted a extensive research on body centered cubic Fe and the effects of elemental additions on its magnetic properties. He showed that the addition of non-magnetic elements such as V, Cr, and Al, resulted in significant magnetostrictive increases over pure Fe [19, 20]. Clark et al. expanded upon Hall's efforts by investigating another non-magnetic elemental addition to Fe, i.e. Ga [1, 15–17, 21–23]. They discovered that upon substituting up to ~20 at% Ga for Fe in the bcc lattice, a ten-fold increase in the tetragonal magnetostriction, λ_{100}, above the magnetostriction of the pure α-Fe was found. As shown in Fig. 1, several unique features characterize the enhanced magnetoelastic behavior of the $Fe_{100-x}Ga_x$ system. These include: (1) a quadratically increasing value of the magnetostriction (3/2) λ_{100}, reaching 400 ppm, with increasing Ga content, up to about $x = 20$ in the bcc solid solution; (2) an absence of the low-temperature maximum in the magnetostriction that is observed in pure α-Fe; (3) a dramatic softening of the shear modulus with increasing Ga content; (4) a decrease in the magnetostriction above $x \approx 20$ and then the appearance of a second peak in the magnetostriction near $x \approx 29$; and (5) a sign change in λ_{111} near $x \approx 19$, where λ_{100} reaches its first apex as shown in Fig. 6. Theories behind why the iron-lattice responds in this manner are yet to be verified experimentally.

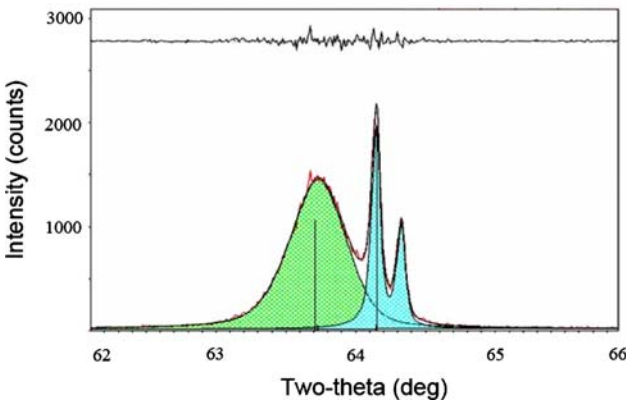

Fig. 5 High resolution XRD scan and profile fit for the 64° reflection in the Fe–19.5 at% Ga sample in the slow cooled condition showing the primary peak splitting attributed to the presence of both A2 and $D0_3$ phases [18]

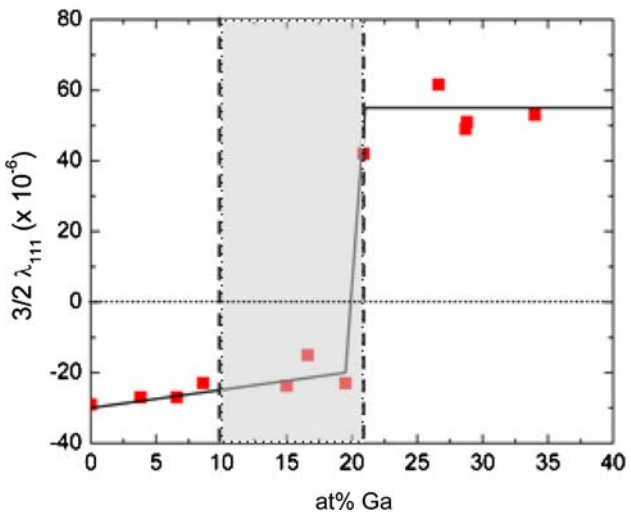

Fig. 6 Magnetostriction constant along the ⟨111⟩ direction in Fe–Ga alloys as a function of Ga content taken from Ref. 1. Note the unique sign change in magnetostriction at ~19 at% Ga

Type I $Fe_{100-x}Ga_x$ Alloys ($0 < x < \sim 19$ at% Ga)

Alloys within this Type I group exhibit the body-centered cubic α-Fe crystal structure, and extend from 0 at% Ga up to ~17 at% Ga independent of thermal history. This compositional limit corresponds to the solubility limit of Ga in Fe. Single crystal X-ray diffraction studies by Lograsso et al. [14] have shown the compositional limits are associated with $D0_3$ phase formation and can be extended upto ~19 at% Ga in quenched samples, where the bcc structure can be retained. Over this same composition range, measurements of the elastic constants by Wuttig et al. using pulse echo techniques [24] and by Clark et al. using resonant ultrasonic spectroscopy [1, 25] found a 2.5 times decrease in the shear modulus, $C_{11}–C_{12}/2$, as shown in Fig. 7. Since the magnetostriction increases quadratically and $\lambda_{001} = -2b_1/3c'$, where b_1 is the magnetoelastic coupling factor, the increase in λ_{001} cannot be accounted for solely by the linear softening of the alloy and a significant increase (>4x) in the magnetoelastic coupling factor is found (see Fig. 8). The magnetoelastic coupling factor has an apparent maximum at $x = 19$ [1]. It is proposed that the Ga atoms form Ga–Ga clusters or pairs and the number of these pairs increases in the disordered (α-Fe phase) bcc structure as the Ga content is increased creating elastic and magnetoelastic defects in the alloy [24]. However, as the Ga content is continually increased ordered structures, $D0_3$ and B2, begin to form reducing the number of pairs, thus reducing the number of defects present in the lattice.

Clark et al. [26] measured the temperature dependences of the magnetostriction constant, (3/2) λ_{100}, anisotropy (K_1), and saturation magnetization (M_s), of $Fe_{91.4}Ga_{8.6}$. Figure 9 compares these data with those of pure Fe [27, 28]. The temperature dependence of the magnetostriction of Fe is very unusual, having a peak near 200 K. Unlike the magnetostriction, the magnetic anisotropy and magnetization of both Fe and Fe–8.6 at% Ga decreases with increasing temperature over the entire temperature range. For Fe–8.6 at% Ga, the magnetization is about 2 T at all temperatures and the values of K_1 increased approximately to 90 kJ/m^3 at low temperatures. The magnetostriction of Fe–8.6 at% was found to increase fourfold to ~110 ppm above pure Fe; however, the magnetostriction still retains an anomalous increase in value with temperature with an apparent peak near room temperature (RT). Surprisingly, the magnetic anisotropy is nearly double that of pure Fe, ~90 kJ/m^3 at low temperature and ~70 kJ/m^3 at room temperature. The large value at room temperature is consistent with the value of ~ 65 kJ/m3 reported by Rafique et al. [29] for Fe–5 at% Ga. The magnetization has decreased about 10% below that of Fe in agreement with the early work of Kawamiya et al. [11] at higher Ga content.

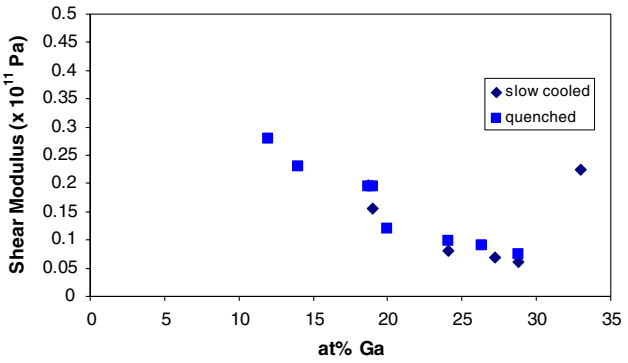

Fig. 7 Plot showing the decreasing $(C_{11}–C_{12})/2$ shear modulus with increasing Ga content in Fe–Ga alloys. Data replotted from Refs. 24 and 25

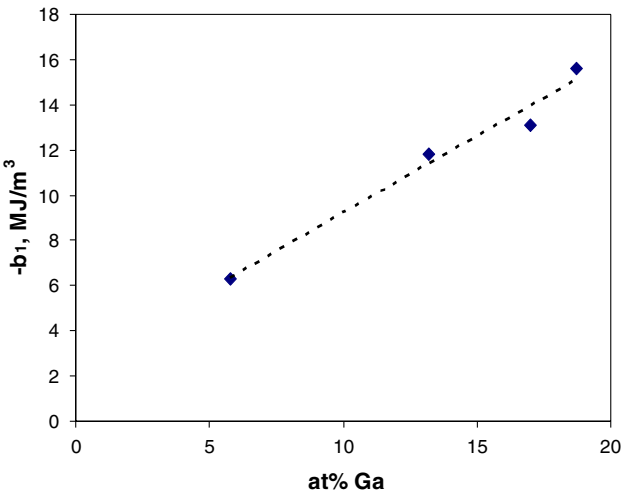

Fig. 8 Plot showing the variability in the magnetoelastic coupling factor, b_1, as a function of Ga content in Fe–Ga alloys. A maximum coupling of 15.6 MJ/m^3 is found at 18.7 at% Ga content. Data plotted from Ref. 1

Mixed Type and Type II alloys (19 at% $< x <$ 29 at% Ga)

While the structural, magnetic, and elastic properties of Type I alloys have been studied with some detail, Mixed Type and Type II alloys have not received the same level of attention. In the mixed region magnetostriction drops off suddenly with the formation of the long-range ordered $D0_3$ phase [14] and reaches a minimum value at ~23 at% Ga [1]. This composition range corresponds with the two-phase region in the metastable phase diagram. However, due to the crystallographic similarities of disordered bcc and ordered $D0_3$ phase, characterization of the phase distribution by X-ray scattering has been limited and no direct

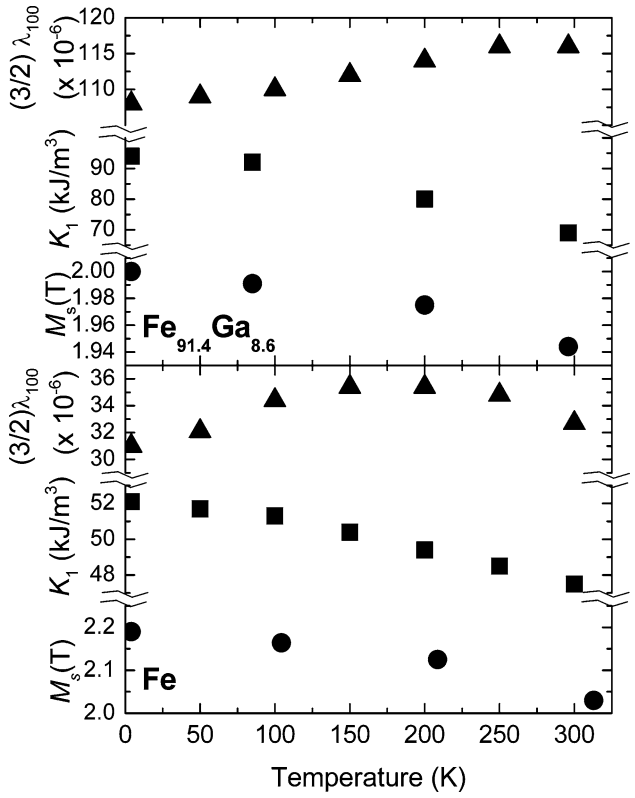

Fig. 9 Temperature dependences of the magnetostriction constant (3/2) λ_{100}, anisotropy (K_1) and saturation magnetization of (M_s) of Fe and $Fe_{91.4}Ga_{8.6}$ from Clark et al. [26]

correlation of the magnetoelastic behavior with structure has been made. Curiously in this composition range, the orthorhombic strain, λ_{111}, reverses sign, increasing from approximately –20 to +60 ppm strain, shown in Fig. 6 [1]. The tetragonal magnetoelastic constant, b_1, falls in magnitude while the rhombohedral constant, b_2, increases in magnitude. The temperature dependence of magnetostriction of Mixed Type alloys also reverts back to anomalous behavior showing positive temperature dependency. Clark et al. [1] suggested that, this unusual behavior is a fundamental behavior of Fe–Ga alloys, speculating long-range $D0_3$ order is detrimental to magnetoelastic coupling [14, 30].

From 24 at% Ga to 29 at% Ga (Type II alloys), the magnetostriction increases again monotonically to a second maximum of equal strain value as the first maximum [1], shown in Fig. 1. Considering the metastable phase diagrams these alloys fall into a single phase $D0_3$ region and the magnetostriction is no longer dependent on thermal history. The increase in magnetostriction has been related to the continued decrease in the shear modulus [1] while the tetragonal magnetoelastic constant remains relatively unchanged. The temperature coefficient of magnetostriction reverts back to negative values and, amazingly, the magnetostriction almost doubles on cooling reaching peak values of ~800 ppm strain at 4 K [26].

Similar large increases in magnetostriction have also been observed in Fe–Al alloys but to a lesser degree with a maximum occurring very near the solubility limit of disordered bcc α-Fe as in Fe–Ga. Figure 1 compares the magnetostriction of Fe–Ga [1,25] and Fe–Al alloys [19]. Based on the analogous magnetostrictive behavior, it has been proposed that the increase in magnetostriction above that of pure Fe occurs as the lattice of Fe is strained along [100] directions due to the emergence of directional short-range ordering of Ga atoms [24]. Note that the concentration dependence of λ_{100} in $Fe_{100-x}Ga_x$ is similar to that of $Fe_{100-x}Al_x$. This behavior is thought to be due to the presence of clusters of solute (Ga or Al) atoms which act as both elastic and magnetoelastic defects. A simple thermodynamic model proposed by Wuttig et al. [24] predicts that at small concentrations, the saturation strain should increase as the number of Ga–Ga or Al–Al pairs increase, i.e., as x^2. For larger x, it becomes impossible to retain the disordered bcc structure, as the alloys become partially or fully $D0_3$ ordered. Measurements of λ_{111} vs. x, for either $Fe_{100-x}Ga_x$ or $Fe_{100-x}Al_x$ show little or no increase with x (for $x < 19$), in contrast to the behavior of λ_{100} [15, 22]. This difference is accounted for, by assuming that there can be no nearest neighbor pairs of Al or Ga, because of the size differentials between Fe and either Ga or Al. In this case, there is no defect-driven contribution to λ_{111}.

Too date, there are no published reports of direct experimental evidence for clustering of Ga atoms although experimental and theoretical evidence is building to support this concept. Viehland et al. [31] has examined single crystal $Fe_{81}Ga_{19}$ using reciprocal lattice mapping and found that (1) the average crystal structure is cubic, with a domain-averaged monoclinic limiting symmetry; (2) structural non-uniformity exists along both the [110] and [001]; and (3) orthorhombic structural modulations exist with a short lateral correlation length. These lattice distortions are indicative of a non-uniform distribution of Ga within the Fe lattice but there are no clear answers even for basic questions, such as, how Ga atoms are incorporated into the Fe lattice and how Ga substitutions affect electronic structure and magnetic properties of Fe. Theoretically, Wu [32] examined contributions of various ordered structures to λ_{100}. For Fe_3Ga ($x = 25$), Wu has investigated magnetostriction in three basic simple structures, namely, $D0_3$, B2-like, and $L1_2$ and found that the local B2-like structure plays a key role for the strong positive magnetostriction in FeGa alloys. This conjecture was confirmed through calculations for larger unit cells with $x = 19$. Nonetheless, the B2 structure is either unstable under tetragonal distortions (for $x = 25$) or is much higher in energy than other phases (for $x = 19$).

Influence of ternary additions—polycrystalline materials

Substantial research has been conducted on ternary additions to the Fe–Ga, (Galfenol) system. Since Hall [19, 20] showed that small additions of transition metals V, Cr, Mo increase the λ_{100} magnetostriction of pure iron, there has been substantial work to examine if transition metal additions would have the same effect on the Galfenol alloys. Kawamiya and Adachi [33] and Nishino et al. [34] have pointed out that additions of elements with either more or fewer electrons per atom than iron stabilize the $D0_3$ phase, which is conjectured to lower the λ_{100} magnetostriction [14]. Stabilization of $D0_3$ also has been argued to account for a change in sign from negative to positive for λ_{111} as a function of Ga content in the binary alloys [1]. The increased $D0_3$ stabilization may be attributed to the substitution of the ternary atoms on different sites of the $D0_3$ structure. Atoms with electron/atom ratio less than the average Fe_3Ga electron/atom ratio reside on the mixed simple cubic lattice site (Fe I) whereas, atoms with electron/atom ratio greater than the Fe_3Ga electron/atom ratio reside on the pure iron sublattice (Fe II) [33]. In both cases, this increases the difference of the average atomic sizes between the two simple cubic lattices, stabilizing the formation of an ordered phase.

The majority of this work has occurred in single crystal systems with the intent of improving the magnetostrictive performance of the alloy around the first observed magnetostrictive peak by increasing the magnetoelastic coupling, further reductions in shear modulus, or avoidance of ordered $D0_3$ phase formation. However, there are published reports of ternary additions to polycrystalline Galfenol alloys and these will be briefly reviewed before discussing single crystal data.

Al substitutions for Ga for directionally grown polycrystalline Galfenol alloys are discussed in a article by Srisukhumbowornchai and Guruswamy [35]. In this article, Al is substituted for Ga at 5, 10, and 15 at% levels in a $Fe_{80}Ga_{20}$ Galfenol alloy. The resultant effect on magnetostriction is a large decrease when the Al substitution exceeds 5 at%. However, later works by Mungsantisuk et al. on similarly processed materials extended the Al substitution to 10 at% in a nominal $Fe_{80}Ga_{20}$ Galfenol alloy without observing severe degradation in magnetostrictive performance [36, 37]. No explanation was given on, why the additional Al substitution, between 5 at% and 10 at%, did not show the decrease in magnetostriction as was seen in Ref. 35. In addition to the FeGaAl system, Ref. 36 also examined Sn, Si, Ge, Ni, and Co additions to polycrystalline Galfenol alloys. The magnetostriction was severely reduced when 2.5 at% Sn, Si, or Ge substitutions were made for Ga in a $Fe_{80}Ga_{20}$ Galfenol alloy. Ni and Co were substituted for Fe in the same $Fe_{80}Ga_{20}$ alloy and showed major decreases in magnetostriction at 5 at% Ni and 5 at% Co substitutions. Preliminary work was completed on Be substitutions for Ga in a $Fe_{80}Ga_{20}$ polycrystalline alloy in Ref. 37. These results showed only a minor decrease in magnetostriction with 2.5 at% Be (228–216 ppm) and 7.5 at% Be (228–194 ppm) substitutions for Ga.

Bormio-Nunes et al. continued the exploration of Co and Ni substitutions for Fe in a $Fe_{85}Ga_{15}$ alloy and also studied Al substitutions for Ga in the same binary alloy [38]. Ingots of $Fe_{85}Ga_{15}$, $Fe_{78}Co_7Ga_{15}$, $Fe_{78}Ni_7Ga_{15}$, and $Fe_{85}Ga_{10}Al_5$ were prepared through chill-casting into a copper mold. Magnetostriction samples were excised from the center of the chill-cast with measurements resulting in low magnetostriction values (maximum value reported = 75 ppm, $Fe_{85}Ga_{10}Al_5$) for all compositions indicating a very poor texture which was not unexpected from the processing technique used. Finally, research by Dai et al. focused on Co substitutions (7 at% and 10 at%) for Fe in $Fe_{90}Ga_{10}$, $Fe_{88}Ga_{12}$, and $Fe_{83}Ga_{17}$ alloys [39]. They concluded that Co substitutions at the levels investigated, while increasing the Curie temperature and reducing the shear modulus, result in a large decrease in magnetostriction over the $Fe_{83}Ga_{17}$ alloy, 320 ppm versus 90 ppm ($Fe_{76}Ga_{17}Co_7$) for water quenched samples.

In summary, ternary additions to polycrystalline Fe–Ga alloys, in the ranges mentioned, typically resulted in significant decreases in magnetostrictive performance. The two exceptions were Al additions <10 at% and Be additions <7.5 at%. These results would suggest that the Ga addition to Fe results in a very unique magnetostrictive property enhancement.

Influence of ternary additions—Single crystal measurements

From this point forward all discussions on ternary additions to the Galfenol system will focus on single crystal specimens prepared by traditional Bridgman growth processes. After crystal growth the samples were homogenized at 1000 °C for 72–168 h and furnace cooled at a rate of 10 °C/min. Oriented disks ~6.35 mm in diameter and ~3 mm thick were sectioned from larger boules with the [100] direction normal to the disk. In-plane [100] and [111] directions were marked on each disk, respectively, as references for strain gage placement for λ_{100} measurements. Similarly, [110] oriented disks with marked [111] in-plane direction were used for λ_{110} measurements. Magnetostrictions were measured by rotating the disk in a 15 kOe magnetic field applied parallel to the disk surface. Saturation strains were easily achieved through the 15 kOe

magnetic field application. Quenching took place on selected samples after magnetostriction measurement were made in the furnace-cooled condition. Single crystal samples were sealed in evacuated quartz tubes, heated from 800 to 1,000 °C for 4 h and then quenched into water.

This review focuses on the additions of ternary elements which are believed to substitute for either Fe or Ga in the disordered bcc lattice. Preliminary results of magnetostriction measurements on Fe–Ga alloys involving interstitial additions (e.g. carbon) have recently been published [40].

Valence electrons less than Fe (V, Cr, Mn, Mo)

Hall [20] showed that slight transition metal additions resulted in significant improvements in λ_{100} of pure Fe. These results prompted research into transition metal additions to Galfenol alloys in an effort to quantify the effects on magnetostriction in the binary, Fe–Ga system. Transition metals investigated with valence electron less than pure Fe includes V, Cr, Mn, and Mo. Figure 10 shows the measured magnetostriction as a function of Ga content for various levels of additions for the above mentioned elements. A 2nd-order polynomial trend line has been fit through the binary, Fe–Ga (Galfenol) single crystal data to help in judging, how effective the ternary addition was with respect to magnetostriction. In addition, the binary data plotted is for quenched Fe–Ga single crystals which exhibit the largest magnetostriction values. Finally, it is assumed in the plot that all ternary additions substitute for Fe, the best case situation. A substitution for Ga would move the respective data point to the left by the amount of the ternary addition (x at%).

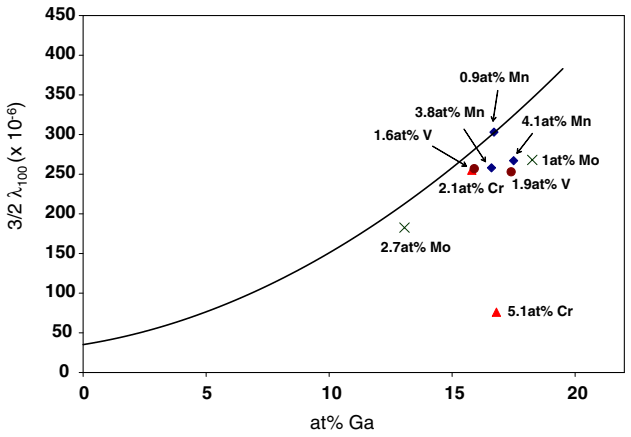

Fig. 10 Magnetostriction constant (3/2) λ_{100} versus Ga content for Fe–Ga–X single crystal samples where X contains valence electrons < Fe. A 2nd order polynomial trend line has been fit through the binary Fe–Ga (Galfenol) single crystal data to aid the eye

V and Cr additions were shown to increase λ_{100} in pure Fe by Hall [20]. However, more importantly, V and Cr additions are known to increase the room temperature ductility of FeCo (Permendur) and Fe_3Al alloys. This improvement in ductility increases the deformability of the alloys allowing for shapes to be processed using conventional deformation techniques such as rolling or forging. It is well known that ~2 at% V is added to 49 at% Fe/49 at% Co Permendur in order to improve upon the brittle nature of the Fe–Co alloy allowing for large volume sheet manufacturing via rolling. In a review article written by McKamey et al. [41] on Fe_3Al alloys it was shown that 2 at% Cr addition to Fe–28 at% Al alloy improved the room temperature elongation from 3.7 to 9.4%. This increase was attributed to a reduction in environmental embrittlement (i.e. water vapor interaction—hydrogen embrittlement) through a change of the oxide coating formed when the alloy is exposed to atmospheric conditions. In a study completed by Defense R&D Canada—Atlantic [42] it was shown that Galfenol may indeed be susceptible to this same environmental embrittlement. The tensile strength of 15 at% Ga and 18.4 at% Ga polycrystal samples significantly degraded (~400 MPa before vs. 300 MPa or below) after being charged with 2–4 ppm of H_2.

The potential mechanical property improvements offered by V and/or Cr make it essential to understand the magnetostrictive response to these additions in Fe–Ga–V and Fe–Ga–Cr alloys. Research is currently underway, investigating various rolling methods that will produce Galfenol sheet where ductility plays a critical role in the final product. Figure 10 clearly shows that V and Cr additions, if made, will need to be at levels of 2 at% or less in order to have a minimal effect on the magnetostrictive response. A Cr addition of 5.1 at% resulted in a large magnetostriction decrease of 244 ppm with respect to the binary at that same Ga content.

Mn additions were investigated to complement the Co work that will be discussed in the next section. Mn lies next to Fe on the left side of the periodic table while Co is to the right of Fe. In addition, Mn will go into solution at a few atomic percent levels without forming secondary phases. Mn additions are also used in some low-carbon steels to increase the ultimate strength through solid-solution strengthening and experimental deformation processing research by the authors has indicated that significant strength improvements can be made with slight Mn additions. Figure 10 shows that as the Mn content is increased above 1 at% large magnetostriction decreases occur. However, the $Fe_{82.4}Ga_{16.7}Mn_{0.9}$ sample only has a 17 ppm decrease over the binary Fe–Ga system and would indicate that this ternary addition if kept below 1 at% shows promise as mechanical strengthening addition without sacrificing magnetostrictive response.

Mo additions were made by Restorff et al. [43] to assess the effect of a partially filled d-shell (4 electrons present in the 4d-shell) on the magnetostriction. Ga has a full compliment of electrons in its 3d-shell and Al has no 3d-shell electrons yet both significantly increase the magnetostriction of pure Fe. Additional data on Fe-Ga-Mo alloys, including λ_{111} data, can be found in Refs. 16, 17, and 43. In addition to investigating d-shell effects, Mo is commonly added to other Fe-based alloys to improve strength and hardenability (i.e. mechanical property improvement), typically at a 0.1–0.2 at% Mo level. Therefore it is important to understand the magnetostrictive effects of Mo additions for future polycrystalline work. Figure 10 shows that Mo additions of 2.7 at% and 1 at% result in a 23% decrease in the magnetostriction over the binary Fe–Ga system. Therefore, any Mo additions in future polycrystalline work should be done at <1 at%.

Table 1 summarizes the magnetostrictive effects for the ternary additions described above. This table shows how the magnetostriction of the binary Fe–Ga system is altered by the respective ternary addition. The additions of V, Cr, Mn, and Mo elements all resulted in magnetostriction reductions. Some of these reductions were quite significant, at the levels added. Figure 11, taken directly from Ref. 40 clearly shows that as Cr and Mn are added the change in sign of (3/2) λ_{111} is shifted left indicating stabilization of the ordered $D0_3$ phase at Ga contents less than the binary system. The stabilization of the ordered $D0_3$ phase would result in a lowering of the (3/2) λ_{100} magnetostriction as is observed in the reviewed research.

Valence electrons greater than Fe (Co, Ni, Rh)

Transition metals investigated with valence electrons greater than pure Fe include Co, Ni, and Rh. Figure 12 shows the measured magnetostriction as a function of Ga content for various at% additions for the above mentioned elements. As before a 2nd-order polynomial trend line has been fit through the single crystal data to help judge how effective the ternary addition was with respect to magnetostriction. In addition, it is assumed in the plot that all ternary additions substitute for Fe. A Ga substitution would move the respective data point to the left by the amount of the ternary addition (x at%).

Co additions complement the work completed on the Fe–Ga–Mn alloys discussed in the previous section. Similar to Mn, Co lies next to Fe on the periodic table and its effects on magnetostrictive properties for single crystal specimens were assessed in Ref. 43. Additions of 1 at% Co

Table 1 Summary of ternary additions to the Fe-Ga system with number of valence electrons < Fe and the change (Δ) in magnetostriction between the ternary and the binary system

Ternary Addition	Binary, Ga content in at%	Δ Magnetostriction, ppm
1.6 at% V	*16*	*–41*
1.9 at% V	*17.5*	*–78*
2.1 at% Cr	*16*	*–43*
5.1 at% Cr	17	–244
10.5 at% Cr	*15*	*–272*
0.9 at% Mn	17	–17
3.8 at% Mn	*16.5*	*–51*
4.1 at% Mn	*17.5*	*–67*
1 at% Mo	18.4	–84
2.7 at% Mo	13.2	–54

Italicized numbers indicate interpolation between existing data points

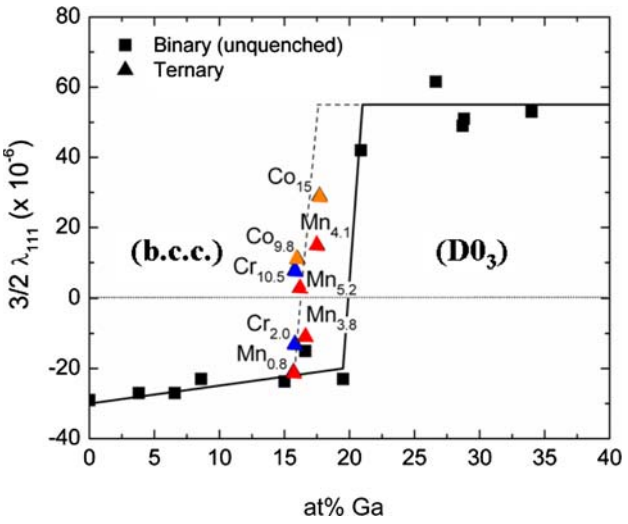

Fig. 11 Magnetostriction constant (3/2) λ_{111} versus Ga content for Fe–Ga–X single crystal samples illustrating the stabilization of the $D0_3$ phase with various alloying additions. Taken from Ref. 40

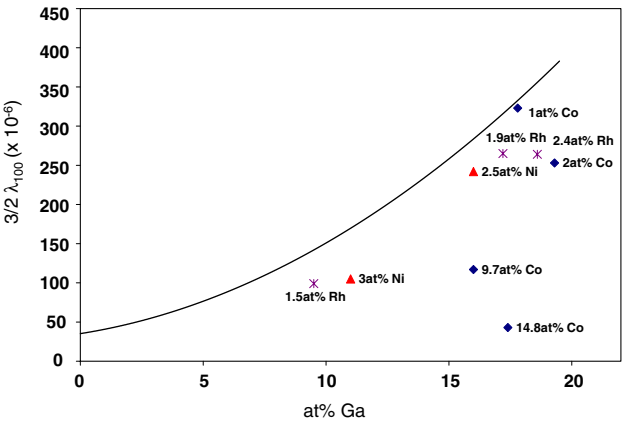

Fig. 12 Magnetostriction constant (3/2) λ_{100} versus Ga content for Fe–Ga–X single crystal samples where X contains valence electrons > Fe. A 2nd order polynomial trend line has been fit through the binary Fe–Ga (Galfenol) single crystal data to aid the eye

to ~15 at% Co were made to binary Fe–Ga samples containing between 16 and 19.3 at% Ga, around the first magnetostrictive maximum according to Fig. 1. Figure 12 clearly shows that as the Co addition is increased, significant reductions in the tetragonal magnetostriction occur. A 1 at% Co addition does not appear to reduce the magnetostriction of the Fe–Ga system, however, an additional 1 at% Co addition results in a 30% decrease in magnetostriction.

Results of Ni additions to the Fe–Ga system were reported on in Refs. 16, 17, and 43. Two Fe–Ga–Ni single crystal alloys were prepared: $Fe_{81.5}Ga_{16}Ni_{2.5}$ and $Fe_{86}Ga_{11}Ni_3$. As stated in the above references, the main purpose of the Ni addition was to decrease the magnitude of the negative λ_{111} in order to reduce the magnetostrictive anisotropy as it does when added to pure Fe as suggested by Bozorth [44]. Measured λ_{111} values for the two samples do show a decrease in magnitude as expected. However, in both cases a large reduction in λ_{100} magnetostriction over the binary system also occurs as shown in Fig. 12; ~19% for the 2.5 at% Ni alloy and ~48% for the 3 at% Ni alloy.

The two magnetostrictive peaks in the binary Fe–Ga system occur close to the single phase A2 region and the single phase $D0_3$ region, respectively, of the metastable phase diagram shown in Fig. 3. It is when two phases coexist (i.e. the A2 and $D0_3$ phases), a large decrease in magnetostriction is measured. The majority of binary Fe–X alloys show the presence of the ordered $D0_3$ phase with one exception being the Fe-Rh system, Fig. 13, which shows no ordered $D0_3$ phase region. Three Fe–Ga–Rh single crystal specimens ($Fe_{89}Ga_{9.5}Rh_{1.5}$, $Fe_{80.9}Ga_{17.2}Rh_{1.9}$, and $Fe_{79}Ga_{18.6}Rh_{2.4}$) were prepared in an effort to improve the magnetostriction through the avoidance of a two-phase region consisting of a disordered and an ordered phase. Unfortunately, Rh additions resulted in a 15–30% decrease in the magnetostriction when compared to the binary Fe–Ga system, shown in Fig. 12. Microstructure examination showed the presence of Rh-rich Fe–Ga–Rh particles present in all samples, Fig. 14. It was determined through EDS analysis that these particles contain 4–10 at% Rh. The exact Fe–Ga–Rh phase has not been identified, and also it is not known to the authors about the effect these second phase particles have on the magnetostriction.

Table 2 summarizes the magnetostrictive effects for the ternary additions with valence electrons >Fe. This table shows how the magnetostriction of the binary Fe-Ga system is altered by the respective ternary addition. Similar to Table 1, large reductions in magnetostriction was seen for Co, Ni, and Rh additions. Figure 11 again shows that Co additions result in a stabilization of the ordered $D0_3$ phase at Ga contents less than the binary system. It is hypothesized that this same response occurs for Ni and Rh additions, thus resulting in lower (3/2) λ_{100} magnetostriction values.

Al and Sn additions to the Fe–Ga system

Al and Sn additions to Fe-Ga alloys were assumed to be substituting directly for Ga atoms and given their atomic sizes would be very unlikely to substitute for Fe. In addition, the electron configurations for Al and Sn are similar with both having un-paired electrons located in p-orbitals (Al–3p1, Sn–5p2) similar to Ga (4p1).

Before the effects of Ga were discovered, Al additions to pure Fe provided the largest increase in magnetostriction

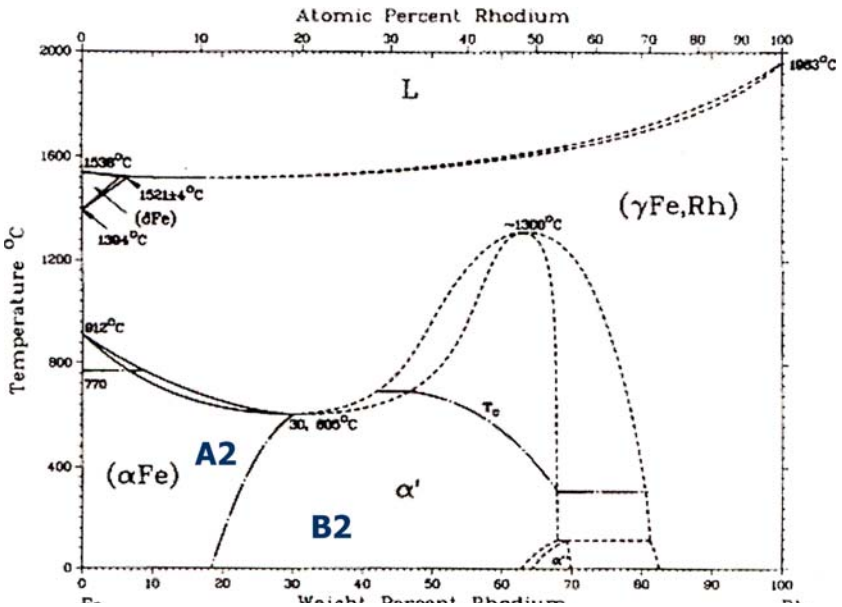

Fig. 13 Fe–Rh equilibrium phase diagram taken from Ref. 6

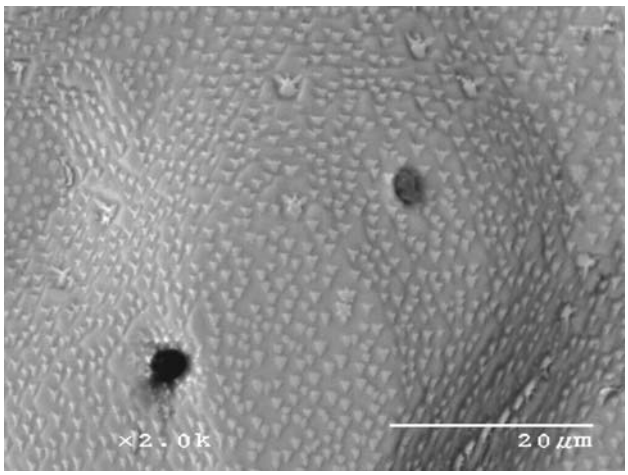

Fig. 14 Fe–Ga–Rh single crystal specimens showing the presence of Rh-rich precipitates (4–10 at% Rh as determined by EDS analysis)

Table 2 Summary of ternary additions to the Fe–Ga system with number of valence electrons > Fe and the change (Δ) in magnetostriction between the ternary and the binary system

Ternary Addition	Binary, Ga content in at%	Δ Magnetostriction, ppm
1 at% Co	*17.8*	*–20*
2 at% Co	19.3	–140
9.7 at% Co	*16*	*–181*
14.8 at% Co	*17.4*	*–290*
2.5 at% Ni	*16*	*–56*
3 at% Ni	*11*	*–73*
1.5 at% Rh	*9.5*	*–40*
1.9 at% Rh	17.2	–55
2.4 at% Rh	18.6	–86

Italicized numbers indicate interpolation between existing data points

for any transition metal, $Fe_{100-x}Al_x$, where $x \sim 15$ [19]. Al substitution for Ga in a Fe–Ga–Al alloy would result in a less expensive alloy as Al is significantly cheaper than Ga and may not adversely affect the magnetostrictive performance. Figure 15 clearly shows that as the Al content is increased in Fe–Ga–Al single crystals the magnetostriction continues to decrease similar to a rule of mixtures behavior. The inset graph in Fig. 15 shows a linear relationship with magnetostriction and Al content as it is increased for $Fe_{87}Ga_{13-x}Al_x$ alloys [19, 22, 43].

It was hypothesized that since Sn has a larger atomic radius than Ga (30% compared to 12%) it will strain the Fe lattice further resulting in increased magnetostrictive values. It needs to be noted that Sn has an extremely low solubility in pure Fe therefore Sn additions were kept to values <2 at%. Five Fe–Ga–Sn single crystal specimens were prepared and through EDS analysis the specimens had the following range

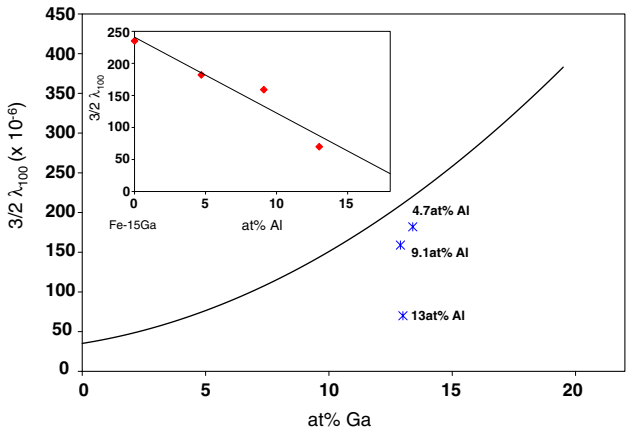

Fig. 15 Magnetostriction constant (3/2) λ_{100} versus Al content for $Fe_{87}Ga_{13-x}Al_x$ single crystal samples

of chemical formulas: $Fe_{81-86}Ga_{12.4-17.6}Sn_{1.4-1.8}$. During the chemical analysis Sn-rich particles (50–80 at% Sn) were noted in the higher Ga content containing samples. Similar to the Fe–Ga–Rh alloys the exact phase has not been identified nor is it known how these particles affect the magnetostrictive response.

Figure 16 indicates that the Sn additions improve the magnetostriction over the binary system. Measured magnetostriction improvements ranged from 0% for the $Fe_{80.8}Ga_{17.6}Sn_{1.6}$ to 18% for the $Fe_{86.2}Ga_{12.4}Sn_{1.4}$ alloy. A water quenching treatment was performed on these specimens in an effort to increase the solubility of Sn in α-Fe, thus improving the magnetostriction. Results of the water quench process are also shown in Fig. 16. The water quench process did not improve upon the magnetostriction, specifically the $Fe_{80.8}Ga_{17.6}Sn_{1.6}$ sample which contains 19.2 at% solute (Ga+Sn) did not show the improvement that the binary $Fe_{80.8}Ga_{19.2}$ composition does. In total, the

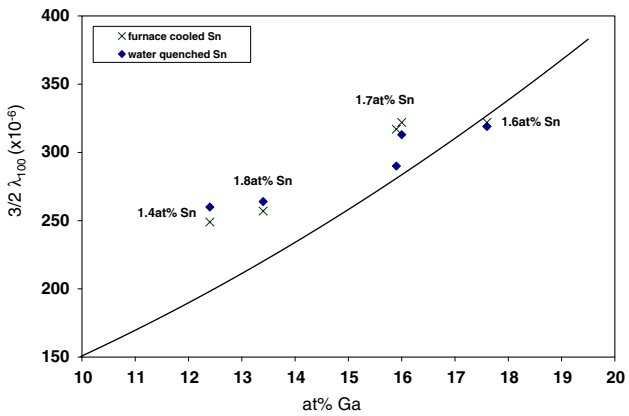

Fig. 16 Fe–Ga–Sn single crystal alloys and the effect of water quenching on the tetragonal magnetostriction. A 2nd order polynomial trend line has been fit through the binary Fe–Ga (Galfenol) single crystal data to aid the eye

Table 3 Summary of Al and Sn ternary additions to the Fe–Ga system the change (Δ) in magnetostriction between the ternary and the binary system

Ternary Addition	Binary, Ga content in at%	Δ Magnetostriction, ppm
4.7 at% Al	13.2	–53
9.1 at% Al	13.2	–76
1.4 at% Sn	*12.4*	*35*
1.6 at% Sn	*17.6*	*–10*
1.7 at% Sn	*16*	*24*
1.7 at% Sn	*15.9*	*22*
1.8 at% Sn	13.4	22

Italicized numbers indicate interpolation between existing data points

water quenching process did not positively or negatively affect the magnetostriction of the Fe–Ga–Sn alloys.

Table 3 summarizes the magnetostriction effects for the Al and Sn additions in Fe–Ga alloys. Al additions appear to result in a linear decrease in magnetostriction appearing to follow a rule of mixtures relationship with Ga additions to Fe. Significant reductions in magnetostriction are seen with Al additions approaching 10 at%. Currently, Sn additions have been the only additions that are able to improve upon the binary Fe–Ga magnetostriction. Magnetostriction increases of 20–30 ppm over the binary have been reported with Sn additions <2 at%. As the Ga+Sn content approached the $D0_3$ phase region ($\sim$19 at% solute) a decrease in magnetostriction below the binary is seen. Further investigations are needed to determine the exact nature of the Fe–Ga–Sn relationship and to understand how Sn is affecting the magnetoelastic elements that drive the magnetostrictive response.

Conclusions

In almost all cases, ternary additions of transition metal elements decreased the magnetostriction values from the binary Fe–Ga alloy. Most of the ternary additions are known to stabilize the $D0_3$ chemical order and could be a primary contribution to the observed reduction in magnetostriction. Alteration of the electronic structure through addition of elements with valence electrons greater or less than Fe does not result in systematic changes in magnetostriction. This insensitivity tends to support the idea that electronic origins of magnetoelastic coupling in Fe–Ga alloys are of secondary importance. In contrast, both Sn and Al are found to substitute chemically for Ga, and for Sn additions, whose solubility is limited, no reduction in magnetostriction strains were observed when compared to the equivalent binary alloy composition and at lower Ga levels increases in magnetostriction were observed with these Sn additions. Aluminum additions, whose effect on the magnetoelastic coupling on Fe is similar to Ga, result in a rule of mixture relationship. The reviewed research suggests that phase stabilization of the disordered bcc structure is a key component to increasing the magnetostriction of Fe–Ga alloys.

Acknowledgements The authors wish to acknowledge support by ONR Code 321MS, ONR MURI Contract N00014-06-10530, ONR Contract No. N00014-05-C-0165, Office of Basic Energy Sciences, Materials Sciences Division, of the U.S. Department of Energy under Contract No. DE-AC02-07CH11358, and the NSWC-CD's In-house Laboratory Independent Research Program.

References

1. Clark AE, Hathaway KB, Wun-Fogle M, Restorff JB, Lograsso TA, Keppens VM, Petculescu G, Taylor RA (2003) J Appl Phys 93:8621
2. Kellogg R (2003) PhD. Dissertation, Iowa State University
3. Kellogg RA, Flatau AB, Clark AE, Wun-Fogle M, Lograsso TA (2003) J Appl Phys 93:8495
4. Kellogg RA, Flatau AB, Clark AE, Wun-Fogle M, Lograsso TA, Russell AM (2003) In: Lagoudas DC (ed) Smart structures and materials 2003: Active materials: behavior and mechanics. SPIE, Bellingham, WA, 5053, p 534
5. Summers E, Lograsso TA, Snodgrass JD, Slaughter J (2004) In: Lagoudas DC (ed) Smart structures and materials 2004: Active materials: behavior and mechanics. SPIE, Bellingham, WA, 5387, p 460
6. Massalski TB (ed) (2004) Binary phase diagrams, 2nd edn. ASM International, Materials Park, Ohio
7. Köster W, Gödecke T (1977) Z Metallkde 68:661
8. Dasarathy W, Hume-Rothery W (1965) Proc R Soc (London) A 286:141
9. Bras J, Couderc JJ, Fagot M, Ferre J (1977) Acta Met 25:1077
10. Ikeda O, Kainuma R, Ohnuma I, Fukamichi K, Ishida K (2002) J Alloys Comp 347:198
11. Kawamiya N, Adachi K, Nakamura Y (1972) J Phys Soc Japan 33:1318
12. Köster W, Gödecke T (1977) Z Metallkde 68:582
13. Gödecke T, Köster W (1977) Z Metallkde 68:758
14. Lograsso TA, Ross AR, Schlagel DL, Clark AE, Wun-Fogle M (2003) J Alloys Comp 350:95
15. Clark AE, Wun-Fogle M, Restorff JB, Lograsso TA, Cullen JR (2001) IEEE Trans Magn 37:2678
16. Clark AE, Wun-Fogle M, Restorff JB, Lograsso TA (2001) In: Hanada S, Zhong Z, Nam SW, Wright RN (eds) Proc fourth Pacific Rim Int. Conf. on advanced materials and processing (PRICM4), The Japan Institute of Metals, p 1711
17. Clark AE, Wun-Fogle M, Restorff JB, Lograsso TA (2002) Mat Trans 43:881
18. Lograsso TA, Summers EM (2006) Mat Sci Eng 416:240
19. Hall RC (1959) J Appl Phys 30:816
20. Hall RC (1960) J Appl Phys 31:1037
21. Guruswamy S, Srisukhumbowornchai N, Clark AE, Restorff JB, Wun-Fogle M (2000) Scr Mater 43:239
22. Clark AE, Restorff JB, Wun-Fogle M, Lograsso TA, Schlagel DL (2000) IEEE Trans Magn 36:3238
23. Cullen JR, Clark AE, Wun-Fogle M, Restorff JB, Lograsso TA (2001) J Mag Mag Mat 226:948

24. Wuttig M, Dai L, Cullen J (2002) Appl Phys Lett 80:1135
25. Petculescu G, Hathaway KB, Lograsso TA, Wun-Fogle M, Clark AE (2005) J Appl Phys 97:10M315
26. Clark AE, Restorff JB, Wun-Fogle M, Dennis KW, Lograsso TA, McCallum RW (2005) J Appl Phys 97:10M316
27. Tatsumoto E, Okamoto T (1959) J Phys Soc Jpn 14:1588
28. (1973) AIP Handbook, 3rd edn. McGraw–Hill, New York, pp 5–145
29. Rafique S, Cullen JR, Wuttig M, Cui J (2004) J Appl Phys 95:6939
30. Bai F, Li J, Viehland D, Wu D, Lograsso TA (2005) J Appl Phys 98:023904
31. Viehland D, Li JF, Lograsso TA, Ross A, Wuttig Manfred (2002) Appl Phys Lett 81:3185
32. Wu R (2002) J Appl Phys 91:7358
33. Kawamiya N, Adachi K (1983) J Magn Magn Mater 31–34:145
34. Nishino Y, Matsuo M, Asano S, Kawamiya N (1991) Scr Metall Mater 25:2291
35. Srisukhumbowornchai N, Guruswamy S (2001) J Appl Phys 90:5680
36. Mungsantisuk P, Corson R, Guruswamy S (2004) In: Chandra D, Bautista RG, Schlapbach L (eds) Advanced materials for energy conversion II. TMS, p 275
37. Mungsantisuk P, Corson R, Guruswamy S (2005) J Appl Phys 98:123907
38. Bormio-Nunes C, Turtelli RS, Mueller H, Grössinger R, Sassik H, Tirelli MA (2005) J Mag Mag Mat 290–291:820
39. Dai L, Cullen J, Wuttig M, Lograsso TA, Quandt E (2003) J Appl Phys 93:8627
40. Clark AE, Restorff JB, Wun-Fogle M, Hathaway KB, Lograsso TA, Huang M, Summers EM (2007) J Appl Phys 101:09C507
41. McKamey CG, DeVan JH, Tortorelli PF, Sikka VK (1991) J Mat Res 6:1779
42. Cheng LM, Veinot D, Fraser P (2006) Quasi-Brittle Fracture in Polycrystalline Galfenol. Study completed for Etrema Products, Inc. through an ONR sub-contract, October 2006
43. Restorff JB, Wun-Fogle M, Clark AE, Lograsso TA, Ross AR, Schlagel DL (2002) J Appl Phys 91:8225
44. Bozorth RM (1951) Ferromagnetism. Van Nostrand, Princeton, NJ, p 667